Metrology for the Micro-Arcsecond Metrology Testbed

Andreas C. Kuhnert, Stuart Shaklan, Yekta Gursel, Steve L. Azevedo, Yao Lin

Jet Propulsion Laboratory, Pasadena, CA, 91109

ABSTRACT

The Space Interferometry Mission (SIM) relies on the combination of interferometry with a metrology system capable of measuring **picometer** relative length changes and micrometer absolute lengths. We are designing the *M*icro-*A*rcsec *M*etrology Test-Bed (MAM) [1] to put these two systems together in a large vacuum tank (12 m long, 2.4 m in diameter). The interferometer has a 1.8 m baseline and is looking at an artificial star 10 m away. The metrology system is measuring the distances between the interferometer mirrors, the interferometer mirrors and the "star" (external metrology), and the interferometer arm lengths (internal metrology). We are using two common path laser heterodyne interferometers to monitor each of these distances. The light sources used are two Nd:YAG lasers with different frequencies, f_0 and f_0+30 GHz. This allows measurement of relative lengths changes as well as absolute lengths. The design for the heterodyne interferometers is in progress using our experience from 1-D and 3-D metrology experiments performed in the past. Modifications include reducing the cross-talk in the internal metrology and adding a polarizing beamsplitter to the laser light path to compensate for path lengths changes caused by temperature changes.

Keywords: interferometer, interferometry, metrology, picometer, heterodyne interferometer

1. METROLOGY MEASUREMENTS IN MAM

The metrology system in MAM is designed to perform the following functions:

1. Measure absolute distances between the interferometer mirrors and between each interferometer mirror and the artificial star, accuracy required ~10^{-6} = 5 μm (external metrology).
2. Measure relative lengths changes in these distances, accuracy required ~10^{-12} = 5 pm (external metrology).
3. Measure relative length changes in the interferometer arms, accuracy required ~10^{-12} =5 pm (internal metrology).

The external metrology measurements are made with respect to two reference points (see figure 1) on the metrology bench. Therefore the distance between these two reference points has to be measured and monitored as well.

In figure 1 the overall scheme of the metrology system in MAMTB is shown. The interferometer measures light from the artificial star at different positions and its internal optical pathlenghts are adjusted to always form the 0^{th}-order fringe, i.e. equal optical path for both arms from the star to the beamsplitter (beamcombiner). The difference in internal optical path (OPD) in the two arms necessary to achieve equal optical path overall can be transformed into an angle with micro-arcsec accuracy for each star position if one knows that OPD to better than 10 pm. This OPD change, when moving the star from one position to the next, is monitored by the internal metrology. The external metrology system in MAMTB monitors the star motion as well; it measures the absolute position of the star before and after it moved and it measures the amount of its motion directly. These measurements are used as an independent measure of the star

motion; we compare them with the interferometric measurement of the star motion to gain confidence in the measurements.

The MAM metrology system measures two dimensions only, i.e. it is not sensitive to small motion in the y-direction (see figure 1). Coplanarity within 300 μm will be achieved by using a theodolite.

Figure 1 Metrology and starlight paths in MAM

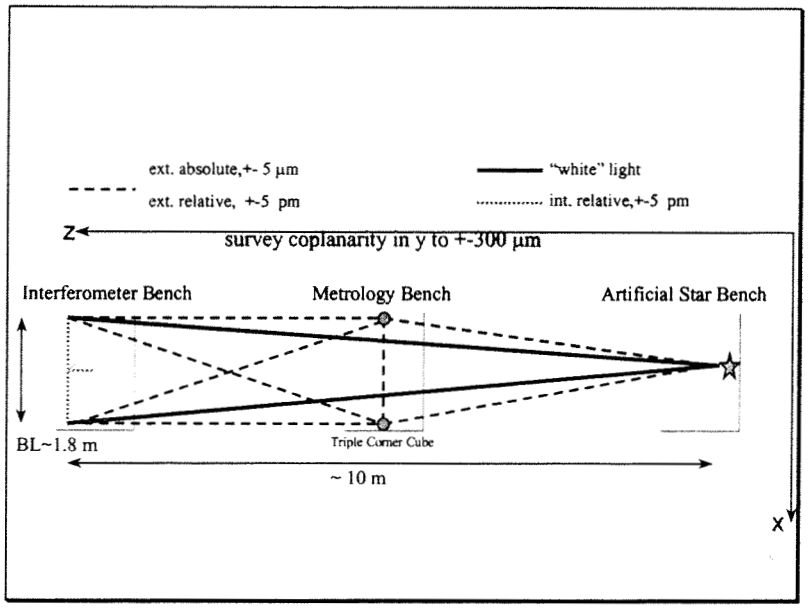

2. METROLOGY GAUGE

The metrology gauges in MAM are heterodyne interferometers [2] measuring the distance change between two retro-reflectors. A heterodyne interferometer consists of a laser source, a beamlauncher, two corner cubes, photodetectors, electronics and the phasemeter. Figure 2 shows this schematically.

The laser source delivers the light at six different frequencies (three pairs, each separated by 10 or 100 kHz, respectively, called heterodyne frequencies), in two orthogonal polarizations and modulated in frequency. This light is fiber-coupled to the beamlauncher assemblies to

1. collimate and combine the two polarizations
2. split light off to create a reference phase signal (beat-signal between the two polarizations).
3. send one of the polarizations onto the round trip between the corner cubes before combining it with the other polarization to create the "unknown" phase signal (beat-signal between the two polarizations).

The photodetector signals are processed in the following way:

1. a DC-coupled pre-amplifier (transimpedance amplifier) converts the photodetector current into a voltage.
2. the sinusoidal signals are filtered to distinguish between the two heterodyne frequencies at 10 and 100 kHz, respectively with band-pass filters (bandwidth approximately 1 kHz).
3. a hysteresis-compensated comparator circuit is used to detect the sinusoid zero-crossings. This circuit triggers a TTL driver on every zero-crossing. The output is a square-wave signal with the rising and falling edges in phase with the sinusoid zero-crossings.

The square-wave signals from both the reference and "unknown" detectors, are the inputs to the lasercard, that is the phasemeter: it measures the phase-difference between the two signals. A change of length between the two corner cubes of $\lambda/2=1319/2$ nm corresponds to a phase-difference of 2π in the round-trip light. This phase-difference in the roundtrip light shifts the phase of the beat-signal by 2π as well.

When measuring distance changes between fiducials (corner cubes) with gauges that utilize light from two lasers (frequencies ν_A and ν_A + 30 GHz) simultaneously for each gauge one can measure the absolute lengths. The phase signals from the two gauges are distinguished by operating them at two different heterodyne frequencies of 10 and 100 kHz, respectively, and then band-pass filtering the signals accordingly. The difference in the phases measured by the two gauges $\Delta\Phi$ is a measure of the absolute distance. This phase difference is modulo 2π, i.e. one needs to know d to the nearest 5 mm (c/(2*5mm)=30 GHz). The absolute distance is this knowledge plus ($\Delta\Phi/2\pi$ * 5 mm).

$$\phi_1 = (4\pi/\lambda_1)*d \qquad \phi_2 = (4\pi/\lambda_2)*d$$
$$\Delta\Phi = \phi_1-\phi_2 = 4\pi*d*(\lambda_1-\lambda_2)=4\pi*d/c(\nu_1-\nu_2)$$
$$d = c/(2*30\ \text{GHz}) * \Delta\Phi/2\pi$$

The metrology gauges that measure the interferometer arm length (internal metrology) suffer cross- talk due to the laser light leaking from one arm into the other at the 50/50 beamsplitter/beamcombiner. This cross-talk is on the order of 1% and it would reduce the accuracy for each arm measurement by adding a signal that corresponds to the length of the other arm. In MAM we avoid this problem by separating the two internal gauges by 200 MHz, i.e. that the beat-signal due to the leakage light is at 200.01 MHz and is filtered out.

Figure 2 Block diagram of a heterodyne interferometer as used in MAMTB.

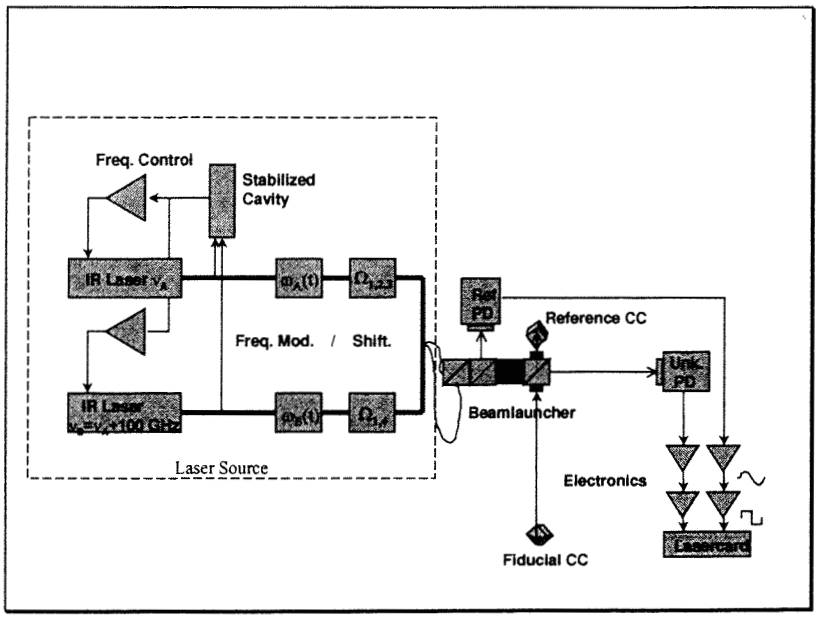

2.1. LASERSOURCE

The laser source for the metrology gauge [3] is shown schematically in figure 3. The two Nd:YAG lasers are operated at frequencies ν_A and ν_B which are different by 30 GHz (100 GHz in future version). They are both frequency stabilized (Pound-Drever-Hall stabilization [4]) to different longitudinal modes of the same optical reference cavity, 5 cm long ULE spacer with mirrors, Finesse ~ 10000, housed in a vacuum

chamber). Figure 4 shows the noise amplitude spectral density of the difference in frequency between the two Nd:YAG lasers (beat frequency), each locked to identical, but independent cavities (any linear drifts are removed).

The light from each laser is modulated in frequency using an acousto-optical-modulator (AOM) in a double-pass arrangement; modulation depth is 86 MHz. It is then split into two orthogonal polarizations. The two polarizations are frequency shifted, using acousto-optical-tunable-filters (AOTF), resulting in different in frequencies [5] (see figure 3). The frequency differences, called heterodyne frequencies, are 10 and 100 kHz, respectively. Throughout the lasersource the light is fiber-coupled from one stage to the next one.

The frequency modulation of the light is necessary to reduce the systematic error in the heterodyne interferometer due to polarization leakage in the beamlauncher [6-8] (caused by: i) misalignment of polarization axes and ii) a finite extinction ratio for S and P polarization in the PBS). This error is periodic with distance changes and leads to a non-linear (sinusoidal) gauge output.

A technique called cyclic-averaging is applied to reduce the magnitude of this error to acceptable levels. The idea behind it is to average over exactly one cycle of this non-linearity. This results in a measurement that corresponds to the true length change, for the periodic non-linearity mean value is zero. There is two different ways of scanning the gauge output over exactly one period of the non-linearity corresponding to one wavelength of OPD (= 1319/2 nm). Moving one of the corner cubes over 1319/2 nm for each gauge individually and integrating the data during the scan is one of them. For MAM we chose to scan (modulate) the frequency of the laser source and integrate the data for a time τ that corresponds to one period of the error. The distance to be monitored by a gauge determines the amount of frequency modulation (modulation depth) that has to be applied for the equivalent of one full wave of motion. MAM's shortest distance monitored is the internal arm length, L ~ 1.8m. With c/2L it follows that changing the laser frequency by ~ 83 MHz corresponds to a 2π shift in the gauge output. In other words, increasing the laser frequency ν by ~83 MHz means that one more wavelength fits into the roundtrip distance. The longer distances L_i need less modulation depth (c/2L decreases with increasing L). Therefore we will use a triangular signal at 100 Hz to modulate the laser frequency by 86 MHz and set the integration times τ_i during this ramp correspondingly for each gauge. The accuracy with which we average over exactly one period of the error determines the suppression factor. A reduction of 1000, which would reduce the error due to polarization leakage from e.g. 2 nm to 2 pm, requires an accuracy of 10^{-3} when determining the integration time. In MAM, counting a 1 MHz clock during the 100 Hz modulation ramp sets the integration time by comparing the clock count to registers that contain the integration times for each gauge. These times will be determined experimentally by looking at the magnitude of the periodic error and minimizing it. During one ramp of 10 ms we collect only 100 samples or less for the various gauges. This limits the accuracy with which we average over exactly one wave of the error to $\geq 1\%$. The required accuracy of 10^{-3} is achieved by phase-locking the clock, ramp and 10 kHz to each other. In other words we make sure that the 1 MHz clock pulses and the 10 kHz zero-crossings coincide with the 100 Hz ramp zero-crossings.

The frequency shifters in the laser source generate the heterodyne frequencies of 10 and 100 kHz, respectively; we are using AOTF's (Bragg-cells) in MAM. Their operating point (efficiency) is around 200 MHz. That is the reason that the laser source output is as shown in figure 3:

1. 200 and 200.10 MHz = 100 kHz heterodyne frequency
2. 200 and 200.01 MHz = 10 kHz heterodyne frequency
3. 400 and 400.01 MHz = 10 kHz heterodyne frequency

The 400 MHz pair, generated by using the AOTF in its full, two-stage configuration, is necessary to avoid cross-talk between the two internal gauges.

Figure 3 Block diagram of laser source

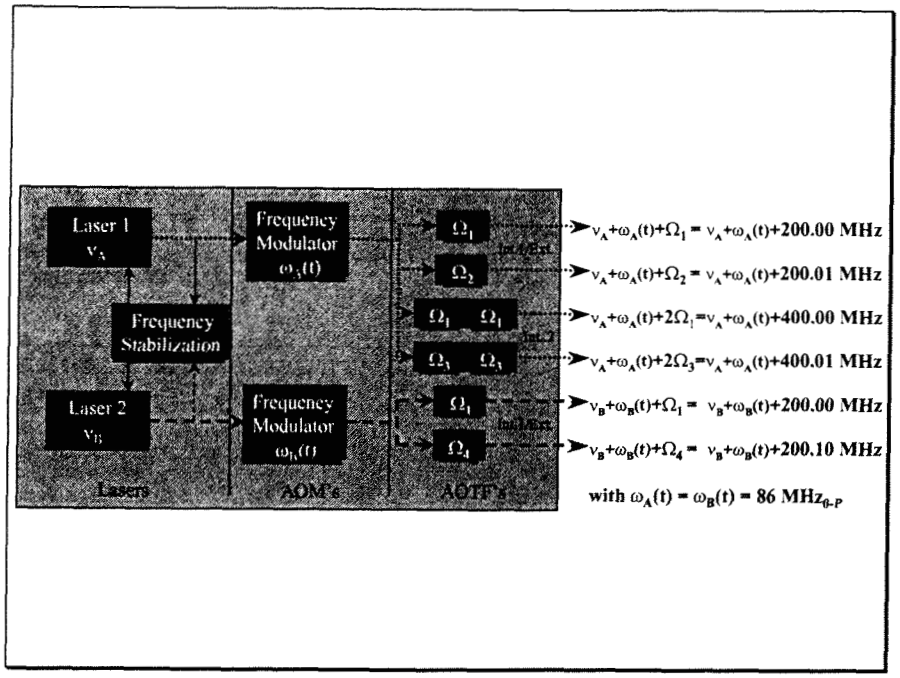

Figure 4 Noise power spectrum of beat-signal between two independently stabilized lasers

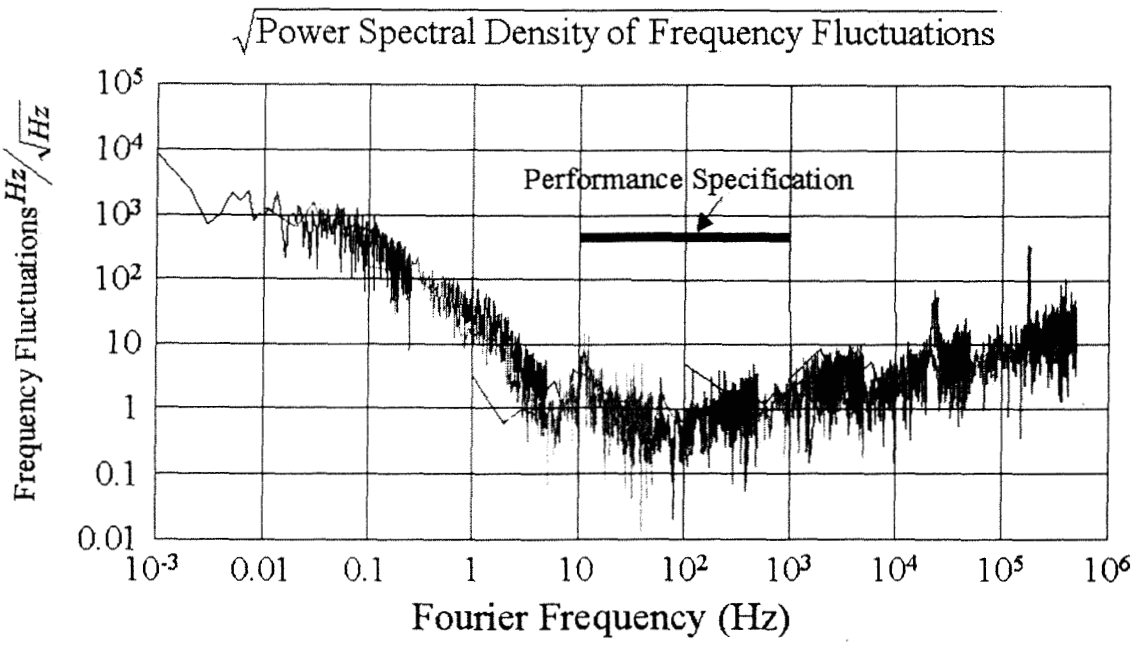

2.2. BEAMLAUNCHER

The light from the lasersource is fiber-coupled with SM/PM-fibers (*S*ingle-*M*ode, *P*olarization-*M*aintaining fibers) to the nine beamlaunchers in MAMTB. A schematic diagram of a beamlauncher is shown in figure 5. The two orthogonal polarizations are aligned so that they correspond to S and P polarized light with respect to the polarizing beamsplitters (PBS). A fiber-collimator followed by a telescope collimates the light to a beamwaist $w_0 \sim 5$mm located just after the telescope. This arrangement was determined experimentally: given the quality and alignment of the optical elements it yielded the best (straightest) fringes at the position of the "unknown" photodetector (figure 6).

After the two polarizations are combined by the first PBS (PBS1) about 10% of the light is split off by a non-polarizing beamsplitter (BS1) to the reference photodetector (RPD). The beat-signal at 10 or 100 kHz from this detector serves as the phase-reference with which the "unknown" photodetector (UPD) beat-signal phase is compared. The rest of the light is split by PBS3: the S-polarized light is sent onto the round-trip between the two corner cubes passing two $\lambda/4$-plates rotating its polarization correspondingly while the P-polarized light goes straight through to the "unknown" detector. A

A second PBS (PBS2), which is rotated about the optical beam axis by 90° with respect to. PBS1 and PBS3, is included to compensate for optical path-length differences in glass between the two polarizations. The two $\lambda/4$ – plates have a high-reflective coating on the outside. The S-polarized component of the light traverses PBS3 three times while the P-polarized light passes through once. With $\delta OP/\delta T = \delta n/\delta T * d + n * \alpha * d$ (T - temperature, n-index of refraction, α - coefficient of expansion (CTE), d=2 cm, the difference in path between S and P-polarized light) we get $\delta OP/\delta T \sim 2.34 * 10^{-7}$ m/°K for BK7 glass. That is ~234 pm for a temperature change of one milliKelvin, which is about the thermal stability that can be achieved over 1 hour inside the vacuum tank. With the rotated PBS2 in place only the temperature gradient between PBS2 and PBS3 is important: the S-polarized component of the light passes this "athermalization" PBS once while the P-polarized light passes it three times, therefore equalizing the S and P paths in glass.

Figure 5 Beamlauncher schematic

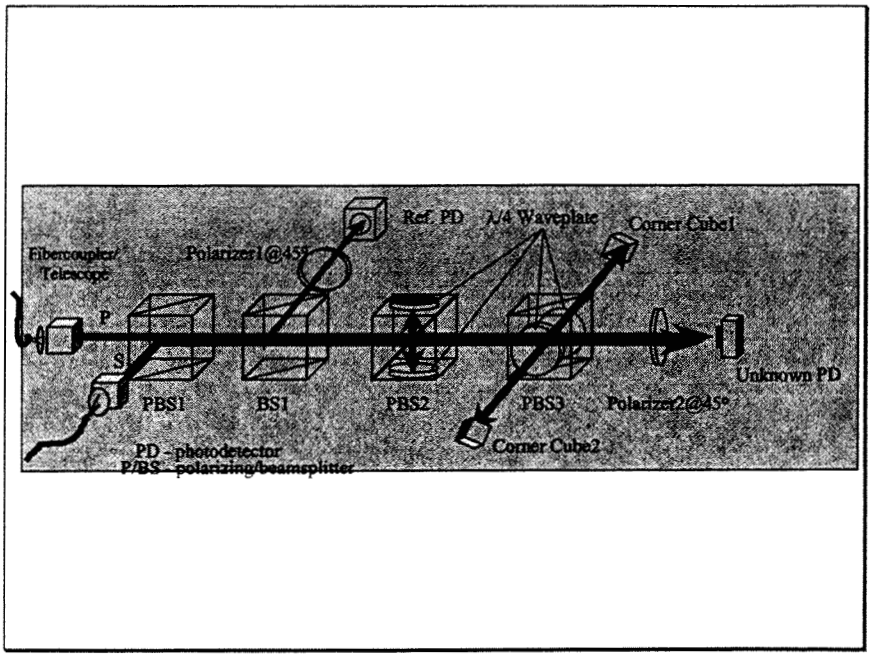

The complete beamlauncher assembly is held by a kinematic piezo-actuator (PZT) stage that is mounted on a motorized stage assembly. This allows for coarse and fine pointing control of the metrology laser beams to the corner cubes. The PZT's also serve as the actuator to dither the beamlauncher so that the laser beam hits the corner cube in a six-point pattern around the true vertex. The response of the gauge is a quadratic function of the pointing-offset from the true vertex, i.e. it is possible to solve for the pointing-offset by finding the minimum in the response. The beamlaunchers are repointed before each measurement to compensate for possible drifts between the measurements. This assures that one measures always to the same point on the corner cubes [9].

Figure 6 Michelson-fringes between the S and P-polarized beam at the "unknown" detector

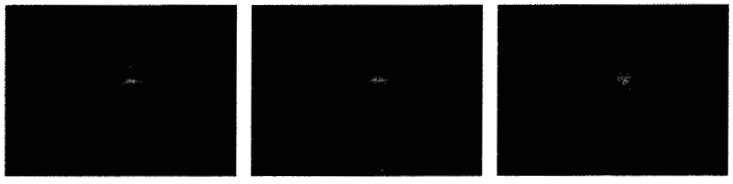

2.3. TRIPLE CORNER CUBE

In MAM the external metrology measurements to the interferometer mirrors and to the artificial star have to be made w.r.t. a common reference, i.e. a common corner cube. The difficulty is that the field-of-view (FOV) for a corner cube is about 60° which makes it impossible in the MAMTB geometry to use a single corner cube as a reference for all the measurements (see figure 1).

We developed a corner cube with a FOV close to 150° [10] by combining four prisms so that they form three corner cubes that have the same vertex (figure 7). The non-common-vertex error is less than 2 μm and the angles are accurate to about 1 arcsec.

We use two of these triple corner cubes forming the metrology bench in MAM (see figure 1). This allows us to measure all distances with respect to their location, and the distance between them results in a complete set of metrology measurements to link everything together.

2.4. LASERCARD

The signals from the metrology gauge photodetectors contain the information about the monitored lengths in their respective phase. The accuracy with which one can measure the lengths depends on how well one can measure these phase differences, i.e. how well one can split one wavelength. In MAMTB this "fringe-splitting" is done with the so-called integrating lasercard. Figure 8 shows the schematic of the lasercard.

Figure 7 Triple corner cube (TCC) as used in MAMTB. The white lines indicate the different light paths into the three corners, which share a common vertex.

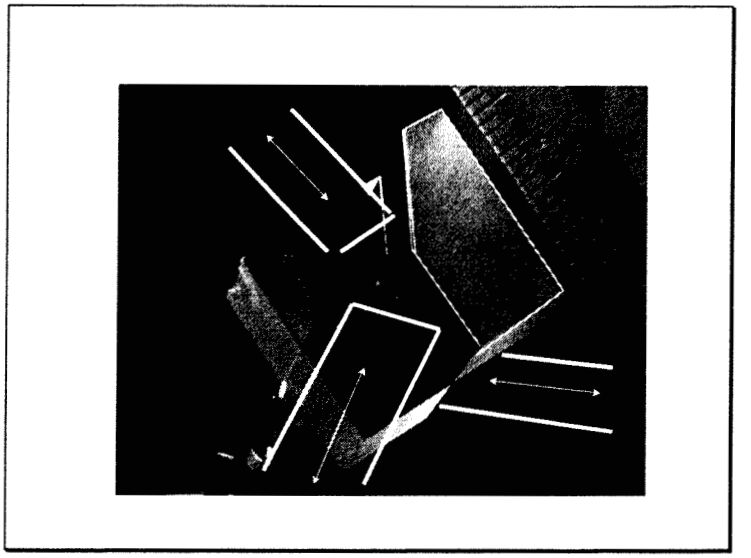

The signals from the reference and "unknown" photodetectors are the inputs to the lasercard (after filtering and square-wave generation). A 128 MHz oven-stabilized crystal oscillator (256 MHz in future version) is serving as the master-clock. This clock is used in two ways:

1. as a counter of the fractional phase difference between the reference and "unknown" signal from each gauge: the reference signal starts the counter while the "unknown" signal stops the counter.
2. as the frequency reference for all MAMTB system specific frequencies to maintain phase-locked synchronization where necessary (see 2.1.). This is achieved by dividing the 128 MHz clock frequency.

The outputs of the lasercard are the number of full-waves-of-motion, the fractional phase difference between the reference and "unknown" signals, and the sum of n measurements integrated over a specified integration time together with the number of measurements (points) that are included in this integral.

The frequency of the reference and "unknown" signals is 10 and 100 kHz, respectively, i.e. the clock count during one full signal cycle (= 1319/2 nm of motion) is 12800 and 1280, respectively. Therefore the immediate accuracy of the gauge is 1319/2 nm/12800 ~ 52 pm and 1319/2 nm/1280 ~ 520 pm, i.e. one full wave-of-motion is split into 52 or 520 pm bins. This is more than the 5 pm accuracy required for the gauges. However, in the presence of random noise on the order of 26 pm (1/2 σ) and averaging over 100 samples (0.01 sec @ 10 kHz) we get 5.2 pm instantaneous resolution when using the 10 kHz gauge for the relative measurements. In the absence of large enough random noise the resolution of our gauges is still sub-picometers. This is because of the frequency modulation for cyclic averaging; it corresponds to a corner cube motion of 660 nm (~ 44000 σ) in 10 ms (100 Hz) during which we take 100 (10 kHz) or 1000 (100 kHz) samples.

We decided to use the 10 kHz heterodyne frequency gauges for the relative distance measurements in MAMTB because we get the better instantaneous resolution while still collecting enough samples for cyclic averaging.

Figure 8 Lasercard functional schematic

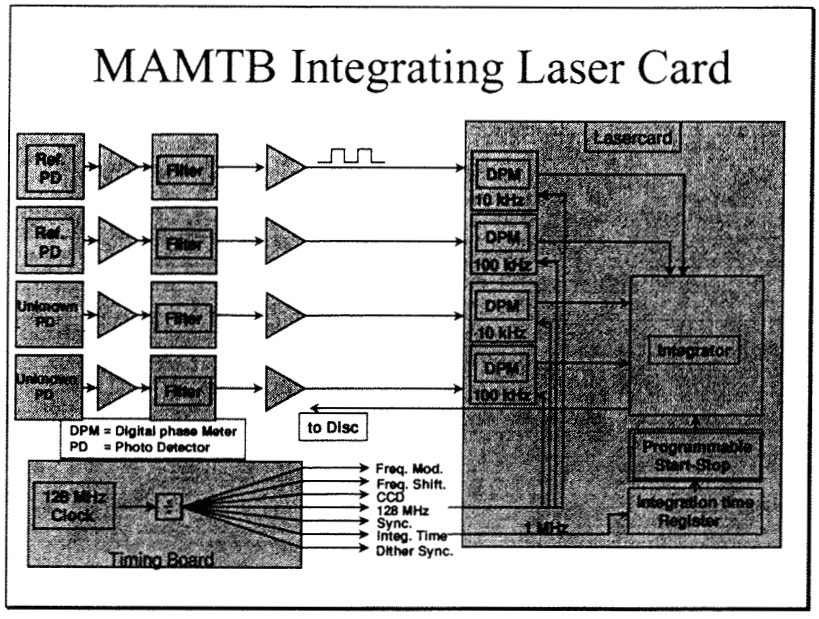

3. CONCLUSION

We are currently in the process of assembling MAM in its intended configuration after the majority of the MAM subsystem parts have been delivered to us. In a first step MAM subsystems like the metrology subsystem will be assembled in air inside the vacuum chamber. By that time all the metrology subsystems as discussed in this paper have been tested to assure their performance. Once assembled we will align the various parts of the metrology system that includes testing the various actuators and their drivers. In parallel to this effort the software to read and process the metrology data is being developed [11].

4. ACKNOWLEDGEMENT

The research described was performed at the Jet Propulsion Laboratory/California Institute of Technology, under a contract with the National Aeronautics and Space Administration.

5. REFERENCES

1. Shaklan, S. et al, Micro-arcsecond metrology testbed, *Proceedings of SPIE International Symposium on Astronomical Interferometry*, ed. R. Reasenberg, Vol. 3350, March 20th – 28th, 1998
2. Gursel, Y., SPIE Vol. 2200, (1994), 27
3. Dubovitsky, S. et al, "Metrology source for high-resolution heterodyne interferometer laser gauges", *Proceedings of SPIE International Symposium on Astronomical Interferometry*, ed. R. Reasenberg, Vol. 3350, March 20th – 28th, 1998
4. Drever, R.W.P. et al, Appl. Phys., **B31,** (1993) 97, and
   Zucker, M.E., California Institute of Technology Ph.D. Thesis, 1989
5. Gutierrez, R.C., "Integrated optic frequency shifters for space heterodyne interferometry", *Proceedings of SPIE International Symposium on Astronomical Interferometry*, ed. R. Reasenberg, Vol. 3350, March 20th – 28th, 1998
6. Bobroff, N., Applied Optics, Vol. 26, No. 13, (1987) 2676

7. DeFreitas, J.M., Player, M.A., J. Mod. Opt., Vol. 42, No. 9, (1990) 1875
8. Wenmei, H., Wilkening, G., Prec. Eng., Vol. 14, No.2, (1992) 91
9. Gursel, Y., "Metrology for space interferometry V", *Proceedings of SPIE International Symposium on Astronomical Interferometry*, ed. R. Reasenberg, Vol. 3350, March $20^{th} - 28^{th}$, 1998
10. Schmidtlin, E., "Novel wide field-of-view laser retro-reflector for the space interferometry mission (SIM)", *Proceedings of SPIE International Symposium on Astronomical Interferometry*, ed. R. Reasenberg, Vol. 3350, March $20^{th} - 28^{th}$, 1998
11. Johnson, R. et al, "Real-time control software for optical interferometers: the RICST testbed", *Proceedings of SPIE International Symposium on Astronomical Interferometry*, ed. R. Reasenberg, Vol. 3350, March $20^{th} - 28^{th}$, 1998